Highly accurate intensity factors of pure CO_2 lines near 2 μm

T. A. Odintsova, E. Fasci, L. Moretti, E. J. Zak, O. L. Polyansky, J. Tennyson, L. Gianfrani, and A. Castrillo

Citation: The Journal of Chemical Physics **146**, 244309 (2017); doi: 10.1063/1.4989925
View online: http://dx.doi.org/10.1063/1.4989925
View Table of Contents: http://aip.scitation.org/toc/jcp/146/24
Published by the American Institute of Physics

Highly accurate intensity factors of pure CO_2 lines near 2 μm

T. A. Odintsova,[1,a)] E. Fasci,[1] L. Moretti,[1] E. J. Zak,[2] O. L. Polyansky,[2,a)] J. Tennyson,[2] L. Gianfrani,[1,b)] and A. Castrillo[1]
[1]*Dipartimento di Matematica e Fisica, Università degli Studi della Campania "Luigi Vanvitelli," Viale Lincoln 5, 81100 Caserta, Italy*
[2]*Department of Physics and Astronomy, University College London, London WC1E 6BT, United Kingdom*

(Received 19 May 2017; accepted 13 June 2017; published online 27 June 2017)

Line intensities for carbon dioxide are measured with a novel spectroscopic approach, assisted by an optical frequency comb synthesizer for frequency calibration purposes. The main feature of the spectrometer consists in the exploitation of optical feedback from a V-shaped high-finesse optical resonator to effectively narrow a distributed feedback diode laser at the wavelength of 2 μm. Laser-gas interaction takes place inside an isothermal cell, which is placed on the transmission from the cavity. High quality, self-calibrated, absorption spectra are observed in pure CO_2 samples at different gas pressures, in coincidence with three lines of the R-branch of the $\nu_1 + 2\nu_2 + \nu_3$ band. Line intensities are determined using a global fitting approach in which a manifold of spectra are simultaneously analyzed across the range of pressures between 5 and 100 Torr, sharing a restricted number of unknown parameters. Various sources of uncertainty have been identified and carefully quantified, thus leading to an overall uncertainty ranging between 0.17% and 0.23%. The measured values are in a very good agreement with recent *ab initio* predictions. *Published by AIP Publishing.* [http://dx.doi.org/10.1063/1.4989925]

I. INTRODUCTION

The concentration of atmospheric carbon dioxide is a source of concern worldwide because of its role in the climate change. From arctic ice core samples, it is estimated that its concentration remained nearly stable for thousands of years until the industrial revolution. More precisely, carbon dioxide levels have increased from 280 parts per million (ppm) to 1850 to 400 ppm today. It is well known that atmospheric CO_2 acts as an effective greenhouse forcing agent, and, consequently, its growing concentration is expected to contribute to the global warming of the Earth's environment. The current knowledge about temporal and spatial variability of atmospheric CO_2 is mostly based on *in situ* measurements from networks of surface stations.[1] Nevertheless, sources and sinks of CO_2 can be only quantified with large uncertainties because of the sparseness of these stations.[1] Satellite sensors, instead, are well-suited to provide dense and uniform observations on a global scale.[2,3] There are currently several satellite-based missions dedicated to atmospheric CO_2 concentration measurements. Among them, the NASA OCO-2 mission (OCO standing for Orbiting Carbon Observatory) has been designed to provide column-averaged CO_2 densities with a target precision in the range 0.3%-0.5%.[4] The accuracy of the satellite data can be of the same level, provided that high-quality spectroscopic parameters are available for the CO_2 vibrational bands of interest. In particular, line intensity factors with an accuracy better than 0.5% are urgently needed for the aims of the OCO-2 and other remote-sensing missions. This is the reason why significant efforts have been recently devoted to the issue of highly accurate linestrength determinations in the near-infrared spectrum of carbon dioxide, both theoretically and experimentally.

As widely experienced in many laboratories worldwide, measuring line intensities is not an easy task. Typical uncertainties for extensive measurements based on FTIR spectroscopy or cavity ring-down spectroscopy range from 1% to 10%.[5,6] For accuracy better than 1%, sophisticated lased-based spectrometers have been developed and used to measure CO_2 line intensities. These studies, however, have been limited to a small number of CO_2 vibration-rotation transitions.[7–9] On the theory side, there have been a number of attempts in the last three decades, but only recently an accurate theoretical solution to the problem of CO_2 line intensities has been provided, using quantum mechanical calculations. The nuclear motion problem was solved with a semi-empirical potential energy surface (PES), which provided with energy levels and rotational-vibrational wavefunctions which in turn were used to calculate transition intensities. The dipole moment surface (DMS), which largely determines the accuracy of calculated transition intensities, was calculated with *ab initio* electronic structure methods, discussed elsewhere.[10,11] Error analysis of the calculated transition intensities based on purely theoretical considerations indicated the majority of strong bands have uncertainties smaller than 1%. Indeed, a first experimental validation of these calculations was performed by using frequency-stabilized cavity ring-down spectroscopy at 1.6 μm.[10] The intensity of 27 vibration-rotation transitions of the P- and R-branch of the (30013)-(00001) vibrational band was measured, and an agreement at the 0.3% level was found with the calculated values.[10]

a)Also at Institute of Applied Physics, RAS, Uljanova 46, Nizhny Novgorod, Russia.
b)Author to whom correspondence should be addressed: livio.gianfrani@unicampania.it.

A puzzling situation arises when comparing *ab initio* calculations with high-quality data available for the CO_2 (20012)-(00001) vibrational band at 2 μm. The average agreement with the intensities measured by Casa *et al.* is at the level of 1%, for nine vibration-rotation transitions of the R-branch.[8] This is not satisfactory considering that the estimated 1-σ uncertainty ranged from 0.1% to 0.2% for those measurements. On the other hand, the calculated value for the R(12) line is in agreement within 0.2% with the measurement performed by Wuebbeler *et al.*[9] Stimulated by this controversy, we decided to perform a new experiment to re-measure the intensities of a few components of the R-branch in the 2 μm region.

In this paper, we report on a new experimental method allowing for highly accurate determinations of line-intensity factors. Laser absorption spectroscopy is performed in an isothermal cell by using a distributed feedback diode laser, whose emission width is effectively narrowed by exploiting the optical feedback from a V-shaped high-finesse optical cavity. Since the spectroscopic experiment is performed by using the light transmitted from the resonator, the spectral resolution is limited by the free spectral range (FSR) of the cavity. This latter was accurately measured by using a self-referenced optical frequency comb synthesizer. The main advantage of the method relies in the fact that the molecular line of interest is probed by a narrow laser. This makes it possible to neglect the influence of the laser emission profile on the observed line shape. Furthermore, self-calibrated spectra are obtained, the frequency separation between two adjacent points being exactly equal to the cavity FSR. On the other hand, the limitation arising from the relatively small number of points of the acquired spectra is mitigated by a global fitting approach. In fact, in contrast to previous works,[7,8] in which individual fits were performed, a global analysis has been implemented and applied to fit a manifold of experimental profiles simultaneously across a given range of pressures, sharing a restricted number of unknown parameters.[12] The partially correlated quadratic speed-dependent hard collision model (the so-called Hartmann-Tran profile or HT profile) has been used in the spectral analysis procedure.[13,14] This model is widely judged to be sophisticated enough to capture various collisional perturbations to the isolated line shape.

II. EXPERIMENTAL DETAILS

The experimental setup, which is schematically shown in Fig. 1, is based on a distributed feedback (DFB) diode laser emitting at 2-μm wavelength, effectively narrowed by exploiting the optical feedback from a V-shaped high finesse optical resonator, similarly to what is usually done in the well known OF-CEAS (Optical-Feedback Cavity-Enhanced Absorption Spectroscopy) technique.[15] The laser light transmitted by the optical cavity is injected into an isothermal gas cell. Finally, a comb-assisted frequency calibration unit is used to determine the free-spectral range of the resonator, thus providing highly accurate calibration of the absorption spectra.

A. The optical resonator

The DFB diode laser, with an emission wavelength centered at 2.007 μm at room temperature, is coupled to an optical cavity with a finesse of about 20 000. This latter is mounted in a V-shaped configuration by using three identical plano-concave wedged high-reflectivity mirrors (having a 1-m radius of curvature and a nominal reflectivity of 99.98% and made on 4-mm thick fused silica substrates) separated by a 52.4-cm long stainless steel spacer (UNS S30400, showing a mean linear thermal expansion coefficient of about 15.4×10^{-6} K^{-1} in the temperature range 20-30 °C). The ring-down time of the cavity was measured to be about 20 μs. The mirrors are fixed to the spacer using adjustable mirror mounts equipped with Viton O-rings (1-mm of thickness) to ensure ultra-high vacuum conditions inside the cavity. The laser light was injected into the cavity through a pair of mirrors. The cavity provides selective optical feedback to the DFB laser from the intracavity field when the laser frequency coincides with that of one of the cavity modes. Optical feedback (OF) guarantees a strong reduction in the laser linewidth. Indeed, although in free running conditions the laser is about 2 MHz wide, the action of the OF results in a narrowing of the linewidth to the level of the cavity mode width, namely, about 10 kHz. Important parameters for an effective and efficient OF-locking are represented by the feedback rate and the distance between the laser and the optical cavity, which in turn determines the phase of the light coming back to the laser.[15] The feedback rate is regulated by a proper combination of a half-wave plate and

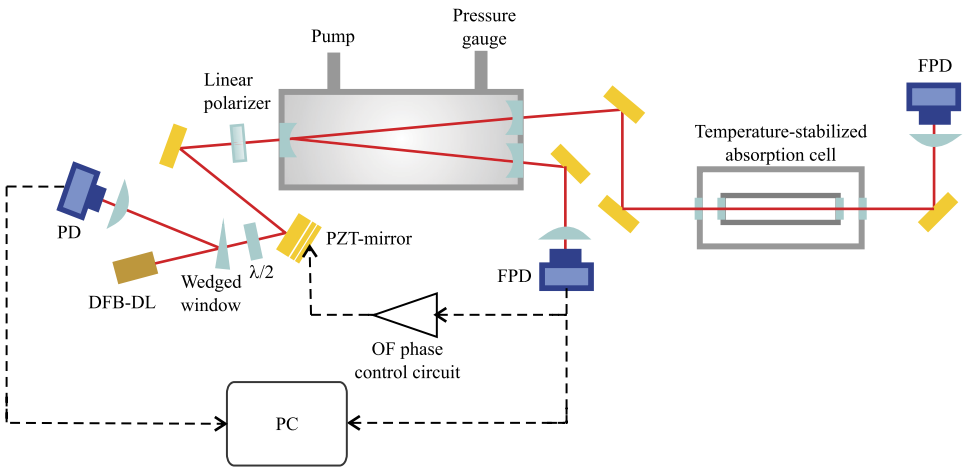

FIG. 1. Sketch of the laser absorption spectrometer. DFB-DL stands for distributed-feedback diode laser, PD for photodetector, FPD for fast photodetector, PZT for piezoelectric actuator, and λ/2 for half wave plate.

a polarizer. As was shown in Ref. 16, laser-to-cavity distance should be about the length of V-cavity arm. Such a distance can be continuously adjusted and optimized (in a real time) by a mirror mounted on a piezoelectric actuator, actively controlled by an electronic feedback circuit.[16] The cavity output is monitored by an extended-wavelength InGaAs photodetector, whose detection bandwidth amounts to about 1.5 MHz. When scanning the laser frequency (at a properly adjusted rate, namely 4 Hz), the symmetry of the each cavity mode is finely quantified so as to produce an error signal that actively controls the distance by piezo-adjustments.

During each laser frequency scan, transient locking of the laser occurs on successive cavity modes. The laser frequency is continuously tuned by acting on its driving current. For a single 14-GHz wide frequency scan, laser passes through roughly 100 cavity modes. As a consequence, the cavity transmission provides a stable and equally spaced comb-like structure in which the frequency distance between two consecutive teeth is determined by the cavity FSR. Finally, the comb is sent to the isothermal cell where the interaction between the frequency-stabilized laser light and the CO_2 gaseous sample can be monitored by another photodetector, identical to the one monitoring the cavity transmission.

The signals provided by the two FPDs, namely the one coming from the high finesse cavity and that emerging from the absorption cell, are simultaneously acquired using a two channels acquisition board (Gage, model CSE1622) having a sample rate of 10^6 Samples/s and a vertical resolution of 16 bit. For each of the two channels, more than 200 000 points can be recorded. A LABVIEW code allows us to control the acquisition card, retrieve the maximum value for each of the cavity resonance recorded by the two detectors and calculate their ratio. The final result is a CO_2 absorption spectrum that consists of about 100 points equally separated by the FSR of the cavity. Examples of acquired signals and retrieved absorption spectrum are shown in Fig. 2. Each spectral acquisition takes less than 1 s. In such a small time interval, any drift of the cavity modes is completely negligible.

B. The isothermal cell

The absorption cell is mounted inside a stainless steel vacuum chamber, which is equipped with a temperature stabilization system as described in details in Ref. 8. Briefly, the cell temperature is measured by a Pt-100 precision platinum resistance (calibrated by the Italian Metrological Institute, INRIM) and kept constant within 0.05 K by means of four Peltier elements driven by a proportional integral derivative controller. This system keeps the gas temperature constant at 296.00 K, with a relative stability better than 0.01% over 5 min and of about 0.02% over a whole measurement run (approximately 8 h). The gas pressure is measured using a 100-Torr full scale capacitance manometer (MKS Baratron, model 690A12TRA) having an accuracy of 0.05% of the reading. A turbomolecular pump is used to periodically evacuate the isothermal cell and create high-purity conditions. A CO_2 gaseous sample with a quoted purity of 99.999% is used in the experiment. An accurate value for the absorption path-length is required for line intensity determinations. Thus, an additional setup for the path-length measurement was implemented and employed, following the approach described in Refs. 8 and 17. Very briefly, the integrated absorbance of CO_2 gas resulting from the absorption cell, A_C, was compared with the one coming from a reference 1-m long cell, A_R. To this purpose, absorption spectra were simultaneously recorded in both cells, when filled with CO_2 gas samples at the same thermodynamic conditions. Each pair of spectra (from reference and isothermal cells) were analyzed using a speed-dependent Voigt profile for the line shape model, so as to retrieve the two values for the integrated absorbance, in coincidence with a given CO_2 line. This procedure was repeated for ten different values of the gas pressure. A linear fit of the integrated absorbance A_C versus A_R gives ratio of the cell length to the reference cell length.

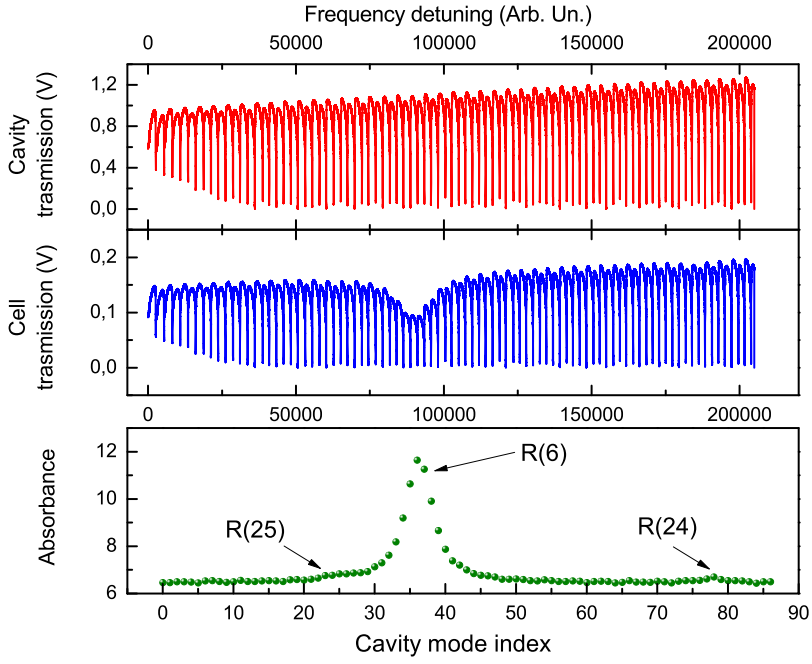

FIG. 2. Transmission signal from the V-shaped cavity (upper plot). The raw spectrum, reported in the middle graph, is given by the transmission signal from the absorption cell, at a wavenumber of about 4983 cm^{-1}. The CO_2 absorption spectrum (lower plot) is retrieved from the logarithm of the peak-by-peak ratio of the two transmission spectra.

Taking into account the value of the reference cell length, as measured by means of a Michelson interferometer,[8] it was possible to retrieve the absorption path-length for the isothermal cell, namely, L = 10.899(6) cm.

C. The frequency calibration unit

In order to produce an accurate frequency scale underneath the absorption spectra, a low-uncertainty measurement of the cavity FSR splitting frequency is necessary. Such a requirement was satisfied by using a self-referenced optical frequency comb synthesizer (OFCS, from MENLO, FC1500-250-ULN), based on an erbium-doped fiber laser. The repetition rate (f_{rep}) and the carrier-envelope offset frequency (f_{ceo}) were stabilized against the frequency of a Rb-clock. The frequency comb provided a supercontinuum in the wavelength range between 1 and 2.1 μm. As it is well known, the absolute frequency of each comb line is given by $f_n = f_{ceo} + n \times f_{rep}$, n being the order of the comb tooth. A second DFB diode laser, identical to the one used for the spectroscopic experiment, was locked to the nearest tooth of the frequency comb by means of proper frequency locking electronics, with an offset frequency of 20 MHz. As a consequence, the frequency of the locked laser, f_{DL}, is equal to $f_{DL} = f_n \pm f_{beat}$, f_{beat} being the frequency offset. It is worth noting that, as widely explained hereafter, the sign of this offset does not enter into the FSR determination. The frequency lock was implemented as follows: A portion of the diode laser beam was perfectly overlapped with the OFCS supercontinuum radiation using three half-wave plates (with a working wavelength of 2 μm) and a pair of polarizing-cube beam splitters, as illustrated in Fig. 3. The first two half-wave plates, mounted on the two arms before the first cube, were used to maximize optical transmission and reflection, respectively. The third half-wave plates and the second cube adjust the polarization of the two overlapped beams. Hence, a grating is used for optical dispersion and selection of the 2-μm radiation, this latter being focused on a fast fiber-coupled photodetector (Thorlabs FPD510) to produce a beat-note signal, which is filtered, amplified, and sent to a servo locking electronics (LLE-SYNCRO Locking Electronics Unit from MENLO). The correction signal from the servo is sent to the laser current driver to actively control the laser emission frequency acting on the current of the laser.

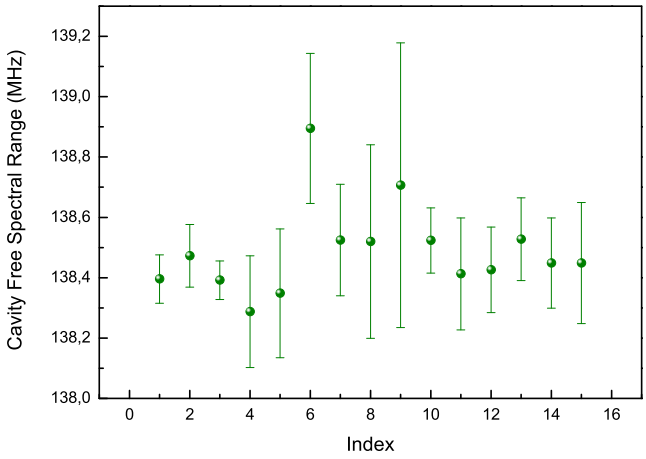

FIG. 4. Determination of the cavity-FSR splitting frequency. Error bars correspond to one standard deviation.

Therefore, highly accurate and reproducible frequency scans of the diode laser frequency could be performed by tuning the comb repetition rate.

The comb-referenced diode laser was coupled to the V-shaped cavity (by using a flipping mirror) and transmission peaks were recorded when tuning the f_{rep}. Hence, the analysis of these spectra (by means of the Airy function) yields the FSR splitting frequency. In Fig. 4, we report the outcomes of 15 sets of measurements, each set consisting of 10 repeated spectra. The weighted mean of these values give a splitting frequency of 138.44 (3) MHz. This FSR value is in full agreement with the one retrieved from the length of the cavity.

III. SPECTRAL ANALYSIS

Absorption spectra corresponding to R(2), R(4), and R(6) components of the (20012)-(00001) combination band of carbon dioxide were recorded at room temperature (T = 296 K) at different gas pressures, in the range of 5-100 Torr. As it is well known, light absorption is ruled by the Lambert-Beer law, namely,

$$\frac{I(\tilde{\nu})}{I_0} = \exp[-S(T)g(\tilde{\nu} - \tilde{\nu}_0)NL], \quad (1)$$

where I_0 and $I(\tilde{\nu})$ are the incident and transmitted power, respectively, N is the molecular number density (in

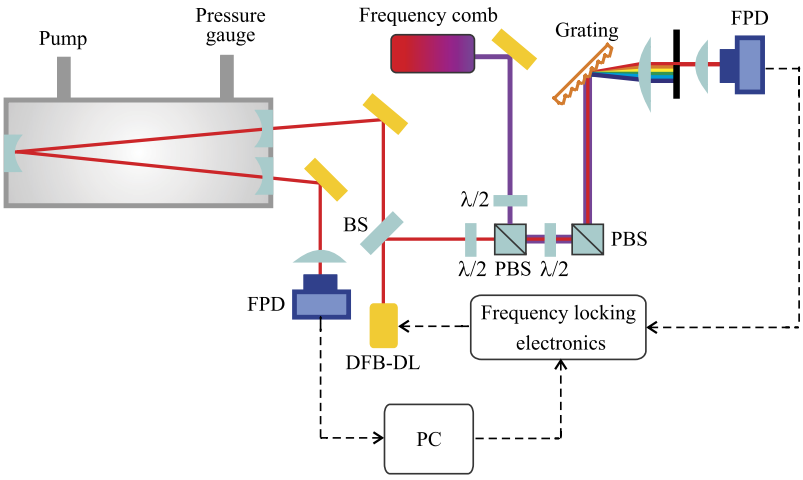

FIG. 3. Sketch of the setup for cavity FSR measurements. DFB-DL - distributed-feedback diode laser, FPD - fast photodetector, BS - beam splitter, PBS - polarizing beam splitter, λ/2 - half wave plate.

molecules/cm^3), L is the absorption path-length (in cm), $S(T)$ is the linestrength (in cm/molecule) at a given temperature, T, and $g(\widetilde{\nu} - \widetilde{\nu}_0)$ is the normalized line shape function (in cm). For a given absorption spectrum, in coincidence with a given vibration-rotation transition, the integrated absorbance is defined by the following integral:

$$A = -\int \ln\left[\frac{I(\widetilde{\nu})}{I_0}\right] d\widetilde{\nu} = S(T)NL.$$

Therefore, a nonlinear least-squares fit of an experimental profile to a given line shape model allows one to retrieve the integrated absorbance as well as other parameters, including the line center frequency and the pressure width.

High-quality determinations of the spectroscopic parameters require a highly accurate and linear frequency scale underneath the acquired spectra and a very refined line shape model accounting for all the broadening and narrowing mechanisms that may affect the absorption profiles. In this work, the use of a comb-calibrated cavity-assisted diode laser absorption spectroscopic technique allowed us to effectively satisfy the first requirement. On the other hand, we adopted the HT profile, that is, a partially correlated quadratic speed-dependent hard-collision profile. It is worth noting that this model, while accounting for the Dicke narrowing effect, the speed dependences of line broadening and shifting, and the partial correlation between velocity- and phase-changing collisions, offers an important advantage with respect to more sophisticated models. The line shape function can be easily and rapidly computed as it is expressible in terms of only two complex probability functions, provided that the speed dependence is considered under the so-called quadratic approximation.[18,19] Very recently, this model has been recommended as universal profile to be adopted for high-resolution spectroscopy in the gas phase.[13] The symmetric version of the HT profile makes use of the following parameters: the line center frequency ν_0, the Doppler width Γ_D, the mean collisional relaxation rate Γ_0, the parameter accounting for the speed dependence of the collisional broadening γ_2, the effective frequency of velocity changing collisions ν_{VC}, and the η parameter representing the partial correlation between velocity changes and rotational-state changes due to collisions. The HT profile can be expressed as follows:[14]

$$\mathrm{HTp}(\nu) = \frac{1}{\pi} Re\left\{\frac{A(\nu)}{1 - [\nu_{VC} - \eta(C_0 - \frac{3C_2}{2})]A(\nu) + (\frac{\eta C_2}{v_{a0}^2})B(\nu)}\right\}, \tag{2}$$

where $A(\nu)$ and $B(\nu)$ are combinations of the complex probability function $w(z)$, according to the expressions here below:

$$\begin{aligned} A(\nu) &= \frac{\sqrt{\pi}c}{\nu_0 v_{a0}}\left[w(iZ_-) - w(iZ_+)\right], \\ B(\nu) &= \frac{v_{a0}^2}{C_2}\Big[-1 + \frac{\sqrt{\pi}}{2\sqrt{Y}}(1 - Z_-^2)w(iZ_-) \\ &\quad - \frac{\sqrt{\pi}}{2\sqrt{Y}}(1 - Z_+^2)w(iZ_+)\Big], \\ w(z) &= \frac{i}{\pi}\int_{-\infty}^{+\infty}\frac{e^{-t^2}}{z - t}dt = e^{-z^2}erfc(-iz). \end{aligned} \tag{3}$$

In these expressions, the quantities X, Y, Z_+, and Z_- are given by

$$\begin{aligned} Z_\pm &= \sqrt{X + Y} \pm \sqrt{Y}, \\ X &= \frac{i(\nu_0 - \nu) + C_0}{C_2}, \\ Y &= \left(\frac{\nu_0 v_{a0}}{2cC_2}\right)^2, \end{aligned} \tag{4}$$

where c is the vacuum speed of light and

$$\begin{aligned} C_0 &= (1 - \eta)(\Gamma_0 - \frac{3\Gamma_0\gamma_2}{2}) + \nu_{VC}, \\ C_2 &= (1 - \eta)\Gamma_0\gamma_2, \\ v_{a0} &= \sqrt{\frac{2kT}{M}}. \end{aligned} \tag{5}$$

In this latter equation, v_{a0} represents the most probable speed of the molecules of mass M at temperature T, while k is the Boltzmann constant. As suggested by Rohart *et al.*,[19] the dependence of the relaxation rates on molecular speed, v_a can be defined by the quadratic function,

$$\Gamma(v_a) = \Gamma_0\left\{1 + \gamma_2\left[\left(\frac{v_a}{v_{a0}}\right)^2 - \frac{3}{2}\right]\right\}. \tag{6}$$

All spectra were fitted to the following function:

$$P(\widetilde{\nu}) = (P_0 + P_1\widetilde{\nu}) + \sum_{i=1}^{n} A^i g^i(\widetilde{\nu} - \widetilde{\nu}_0), \tag{7}$$

where P_0 and P_1 are two parameters accounting for a possible residual variation of the laser power, while the superscript i (varying from 1 to n) indicates the various lines that are considered, including the probed line and the interfering ones. For the aims of the present work, n = 3.

Table I reports spectroscopic data related to the probed and interfering lines. These data are relevant for the spectral analysis.

For each of the lines probed, a global analysis procedure was applied to the experimental spectra, which were recorded at 20 different gas pressures. As demonstrated elsewhere,[21] the advantage of the global analysis is the significant reduction of correlation issues among free parameters. In fact, in this approach, some parameters can be shared among all the spectra, thus providing physical constraints. This is the case of the self-broadening coefficient, γ_0, the γ_2 parameter, the Doppler width, Γ_D, and the η parameter, for each line of any spectrum. The integrated absorbance and the central frequency of the probed line, as well as the baseline parameters, were retained as free parameters in the individual spectra. The effective frequency of velocity changing collisions was fixed for all the lines at the value coming from diffusion theory, $\nu_{VC} = \frac{kT}{2\pi MD}$, which is equal to 0.028 cm^{-1}/atm (namely, 1.09 MHz/Torr), D being the mass diffusion coefficient. As for the parameters of the interfering lines, the frequency detuning from the center of the main line was fixed at the value provided by the HITRAN database,[20] while the integrated absorbance was scaled in comparison to that of the probed line according to the intensity ratio reported in Ref. 11.

TABLE I. CO_2 lines investigated along with their central frequency and their frequency detuning, $\Delta\nu$, from a pair of interfering transitions.[20] The intensity ratios (I_1/I_p and I_2/I_p) of the interfering lines with respect to the probed one are also reported.[11]

Probed line	ν_0 (cm^{-1})	Interfering line	$\Delta\nu_1$ (MHz)	I_1/I_p ($\times10^{-3}$)	Interfering line	$\Delta\nu_2$ (MHz)	I_2/I_p ($\times10^{-3}$)
R(6)	4983.001 149	(21112)-(01101) R(24)	1600.5019	44.30	(21112-01101) R(25)	−5744.2335	42
R(4)	4981.626 214	(21112-01101) R(22)	527.3949	65.45	(21112-01101) P(12), $^{13}C^{16}O_2$	−3136.6086	11.2
R(2)	4980.131 728	(30012-10001) R(30)	774.5138	4.32	(21112-01101) R(20)	−6924.8160	114.24

IV. RESULTS AND DISCUSSION

The global fitting procedure was used to fit simultaneously twenty spectra, recorded as a function of the CO_2 gas pressure. Since 100 repeated spectral acquisitions were performed for each pressure value, the fitting procedure could be applied repeatedly, allowing for analysis of all recorded spectra. Examples of line fitting for a pair of spectral acquisitions at different pressures, for the R(4) line, are reported in Fig. 5. Very good agreement between the experimental data and the theoretical model was found, in these two examples as well as for all recorded spectra. The root-mean-square value of the residuals amounts to about 2×10^{-3}, limited by the experimental noise. No clear structures could be evidenced in the residuals, at any pressure. This demonstrates the capability of the HT profile for modeling the absorption spectra over the entire pressure range. It is worth noting that no asymmetry in the recorded profiles could be evidenced; this is the reason why the speed-dependence of pressure shifting was neglected.

Figure 6 plots an example set of retrieved values of the integrated absorbance (resulting from the application of the global fitting approach) as a function of the molecular number density, for the R(2) line. In calculating the number densities, we took into account the gas pressure, temperature, and purity, as well as the isotopic composition of the sample gas. This latter could be determined by means of isotope ratio mass spectrometry, when applied to a sample taken from the bottle in use. Each point results from the statistical analysis of 100 values, yielding the mean value and the standard deviation. The experimental points were fitted to a straight line by using a weighted total least-squares linear regression,[22] in order to consider the uncertainties on both the absorbance and the number density. A good agreement is found between the experimental points and the best-fit line, the root-mean square (rms) value of the relative residuals being 0.6%. It is relevant to note these determinations were repeated, for each of the investigated lines, in two different days so as to retrieve the linestrength S from a weighted mean of two different and independent set of measurements.

The measured line intensity factors are given in the 2nd column of Table II, along with linestrength values from *ab initio* calculations (3rd column), values from databases (5th and 6th columns), and values from previous experimental studies (7th and 8th columns). The uncertainties in the second column of Table II include type A and type B uncertainties and correspond to 1-σ. The fourth column gives the relative deviations between the present measurements and *ab initio* calculations. The level of agreement is very

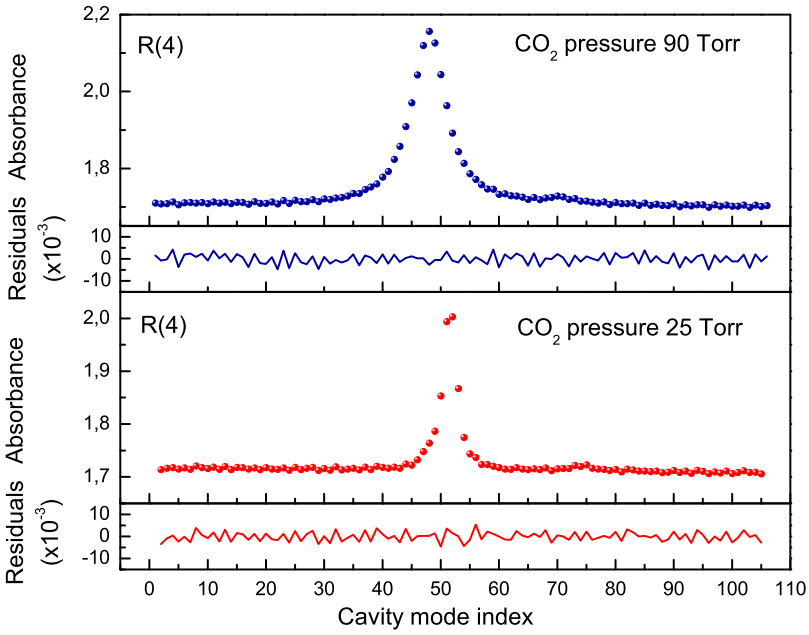

FIG. 5. Examples of absorption spectra for the R(4) line, along with the residuals resulting from the application of the global fitting approach to a set of 20 spectra, across the pressure range between 5 and 100 Torr.

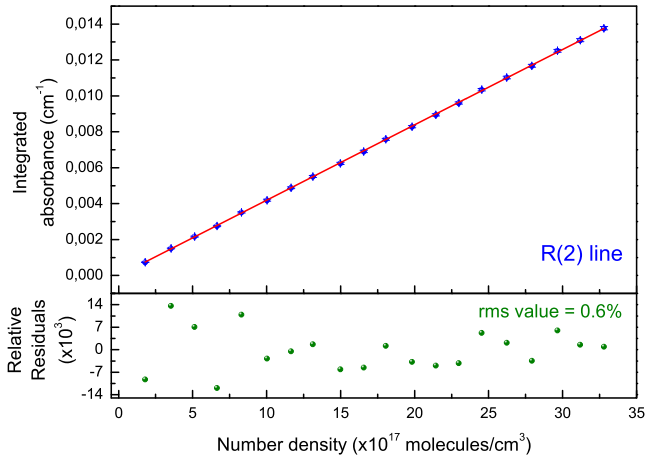

FIG. 6. Plot of the integrated absorbance as a function of the molecular number density. Excellent agreement is found between the line and the experimental points. The slope of the best-fit line provides the quantity SL, from which the line intensity factor can be determined, using the value of the absorption path length of Sec. II B. We draw the reader's attention to the fact that, as expected, the intercept of the best-fit line is well consistent with zero within the experimental uncertainty.

satisfactory, the mean relative deviation being 0.35%. It should be noted that such the deviation increases as J is lowered, probably because of the decreasing signal-to-noise ratio in the recorded spectra. Furthermore, the new experimental values show a relative deviation from those of Ref. 7 of 1.1%, –0.77%, and 1.66%, respectively, for the R(6), R(4), and R(2) lines. Similarly, the relative deviations from the data of Ref. 8 amount to 0.6%, 0.1%, and 1.43%. Therefore, it appears that the data from past experiments are less accurate than expected. We believe that these discrepancies (larger than the quoted uncertainties) are due to the inadequacy of the line shape models adopted in past works.[7,8] In fact, repeating the spectral analysis for the R(6) line by means of individual fits based on the Nelkin-Ghatak profile, we found a linestrength value of 8.23 (6) × 10^{-22} cm/molecule, which is 1.5% smaller than the present value. The same spectra, when analyzed by using the multispectrum approach with the Nelkin-Ghatak profile, lead to a value of 8.245 (12) × 10^{-22} cm/molecule that is still 1.3% smaller. Another source of deviation can be ascribed to the pressure gauges, which were used at that time. In fact, we have discovered that they are much less accurate than the one used in the present work, much worse than their quoted accuracy of 0.25%. A further remark comes from the comparison with the databases. It turns out that the level of agreement is much better for the GEISA values, rather than the HITRAN 2012 database. In particular, the mean deviation amounts to 0.81% for GEISA and 2.94% for HITRAN 2012. It should be noted that theoretical transition intensities from Ref. 11 are included in the recently released 2016 edition of the HITRAN database.[24] As far as the uncertainty budget is concerned, it is useful to remember that the evaluation of type A uncertainties is based on any valid statistical method for treating data, while type B uncertainties (including systematical deviations) are inferred from scientific judgment or other information concerning the possible values of the quantity. The type A uncertainty could be directly inferred from the weighted mean of values resulting from linear fits similar to that of Fig. 6. As stated above, in the linear best-fit procedure we took into account the uncertainty on the integrated absorbance as well as the one on the molecular number density. In particular, the former results from the statistical analysis of 100 values, as retrieved from the global fitting procedure. The latter comes from the combination of two contributions, of type A and type B, related to the temperature measurement (0.02%) and to the accuracy of the pressure reading (0.054%), respectively. It must be noted that the uncertainty on the gas pressure also includes a 0.02% contribution originating from the measurement of the isotopic composition of the gas sample. Finally, from the weighted linear fits, we quoted an overall type A uncertainty in the range between 0.15% and 0.20%, depending on the investigated absorption line.

Type B contributions can be ascribed to (i) the optical path length, (ii) the detector's nonlinearity, (iii) the influence of the line-shape model, and (iv) the FSR uncertainty. The overall component associated to the optical path length resulted to be 0.06%, also in this case a combination of a statistical uncertainty (0.055%) and a type B uncertainty (0.019%) associated to the length of the reference cell.

Regarding the detector nonlinearity, we assumed that the performance of extended-wavelength InGaAs photodiodes was similar to standard-type InGaAs detectors, which show linearity within 0.04% (at one standard deviation) over the photocurrent range from 10^{-7} to 10^{-4} A.[25] In order to quantify its influence on linestrength determinations, we adopted the following procedure: after simulating "nonlinear" absorption spectra, we did the spectral analysis and determined the integrated absorbance, which was compared to the expected one. We found an average relative difference (over the simulated pressure range) of about 6 × 10^{-4}. In a very pessimistic view, the simulated nonlinearity was considered in the form of a frequency-dependent second-order polynomial added to the vertical scale of each simulated spectrum so that the relative

TABLE II. Measured line intensities with their global uncertainty in comparison with values from databases,[20,23] results from recent theoretical calculations[11] and from past experimental studies.[7,8] Line intensities values are expressed in ×10^{-22} cm/molecule and following the HITRAN convention are rescaled to the isotopic $^{12}CO_2$ natural abundance, namely 0.9842.[20]

Line	Present work	*Ab initio* calculations[11]	Relative deviation (%)	HITRAN values[20]	GEISA values[23]	Values from Ref. 8	Values from Ref. 7
R(6)	8.355 ± 0.014	8.348	0.08	8.133	8.309	8.305	8.263
R(4)	6.235 ± 0.012	6.210	0.40	6.049	6.182	6.229	6.187
R(2)	3.844 ± 0.009	3.822	0.57	3.722	3.805	3.789	3.780

deviation between original and distorted spectra was 0.04%. In order to quantify the influence of the adopted line shape model, we numerically simulated CO_2 spectra (in the pressure range 5-100 Torr), in coincidence with the R(6) line, assuming that the line profile is given by a partially correlated speed-dependent hard collision model with a hypergeometric dependence on the absorber speed for both pressure broadening and pressure shifting parameters (pcSDHC-hg). Then, the application of the global fitting procedure, based on the use of the HT profile, to the set of simulated spectra showed that the systematical deviation between retrieved and expected linestrength values was negligible. This is expected on the basis of the outcomes of Ref. 26, where despite the differences between HT and pcSDHC-hg models, the determination of the absorbance resulted to be quite robust, regardless of the choice of the form used to represent the speed dependence. The last source of type B uncertainty can be ascribed to the cavity FSR. Since the free-spectral-range enters into the frequency scale calibration, its uncertainty may influence the accuracy of our linestrength determinations. To this end, we have repeated the overall spectral analysis (global fitting plus weighted linear fits) adopting two different FSR values, at the two edges of the interval FSR $\pm\ \sigma_{FSR}$, where σ_{FSR} is the statistical uncertainty of our FSR determination (namely, 0.03 MHz). So doing, we included 1-σ systematic component of 0.03% in the uncertainty budget for our linestrength determinations. It must be noted that the possible contribution to the FSR uncertainty due a temperature gradient in the cavity spacer can be completely neglected. In fact, a slight variation of the laboratory temperature (at the level of $\pm 2\ ^{\circ}C$) affects the length of the cavity spacer, thus leading to a variation of the cavity FSR. On the other hand, no refraction index effect can be observed as high-vacuum conditions are routinely ensured inside the optical cavity. Because of the small temperature coefficient of the cavity spacer, the relative variation of the cavity FSR does not exceed 3×10^{-5}.

To summarize, the complete uncertainty budget leads to a 1-σ global uncertainty of 0.17%, 0.19%, and 0.23% respectively for the R(6), R(4), and R(2) lines.

The line shape parameters, resulting from the application of the global-fitting approach, are presented in Table III. The values for the partial correlation parameter sound reasonable, being close to the ones retrieved in Ref. 27 for some components of the R-branch of the (300 13)-(000 01) band, using the same line shape model. The quadratic speed-dependence parameter, γ_2, is consistent with an interaction potential of the form $\frac{C}{r^q}$, with the exponent q roughly varying between 5 and 7, the former being typical of a quadrupole-quadrupole interaction, the latter occurring for a quadrupole-induced dipole force. As for the pressure broadening coefficient, we may note a satisfactory agreement with the HITRAN database[20] only for the R(6) line. This is not surprising because of the large uncertainty of the HITRAN values.

TABLE III. Line shape parameters (Γ_0, γ_2, and η) measured in the present work. The pressure broadening coefficient is given in terms of a half-width at half maximum.

Line	Γ_0 (cm^{-1} atm^{-1})	γ_2	η	Γ_0 (cm^{-1} atm^{-1}) HITRAN[20]
R(6)	0.1162 ± 0.0003	0.195 ± 0.006	0.23 ± 0.02	0.114 ± 0.002
R(4)	0.1206 ± 0.0005	0.201 ± 0.008	0.19 ± 0.04	0.116 ± 0.002
R(2)	0.1229 ± 0.0006	0.174 ± 0.012	0.17 ± 0.06	0.119 ± 0.002

V. CONCLUSIONS

This paper describes a comb-calibrated laser absorption spectroscopic method to accurately measure line intensity factors for carbon dioxide at the wavelength region near 2-μm. Significant improvements are reported as compared to past experiments. Firstly, a V-shaped high-finesse optical cavity is used to narrow at the kHz level the emission width of the DFB diode laser that is used to probe CO_2 vibration-rotation transitions of the (20012)-(00001) band. Secondly, the use of a self-referenced optical frequency comb synthesizer ensures a highly accurate frequency scale underneath the absorption spectra. Thirdly, differently from previous works,[7,8] in which individual fits were performed, a global fitting approach has been adopted for the simultaneous analysis of a manifold of experimental spectra across the entire pressure range (namely, between 5 and 100 Torr). In such a procedure, the possibility of sharing some parameters (including the Doppler width and the pressure broadening coefficient) within sets of spectra ensures a significant reduction of statistical correlation issues among free parameters. The so-called Hartmann-Tran profile has been adopted as line shape model. As a result of a detailed budget of uncertainties, the global uncertainty for our linestrength determinations was found to vary from 0.17% to 0.23%. The agreement between our measurements and *ab initio* calculations resulted to be at the level of 0.35%, which is well within the estimated theoretical uncertainties. This comparison provides an important demonstration of the validity of the theoretical procedure for determining CO_2 line intensities for the 2-μm wavelength region.

ACKNOWLEDGMENTS

The authors are grateful to Mikhail Tretyakov for stimulating discussions. This work was partially supported by EURAMET through the EMRP Project No. SIB01-REG4, within the Ink (Implementing the new Kelvin) Project coordinated by Graham Machin, and by UK Natural Environment Research Council under Grant No. NE/J010316. O.L.P. acknowledges the Russian Fund of Basic Research for funding Project No. 15-02-07473.

[1] K. R. Gurney, R. M. Law, A. S. Denning, P. J. Rayner, D. Baker, P. Bousquet, L. Bruhwiler, Y.-H. Chen, P. Ciais, S. Fan, I. Y. Fung, M. Gloor, M. Heimann, K. Higuchi, J. John, T. Maki, S. Maksyutov, K. Masarie, P. Peylin, M. Prather, B. C. Pak, J. Randerson, J. Sarmiento, S. Taguchi, T. Takahashi, and C.-W. Yuen, "Towards robust regional estimates of CO_2 sources and sinks using atmospheric transport models," Nature **415**, 626–630 (2002).

[2] H. Boesch, G. C. Toon, B. Sen, R. A. Washenfelder, P. O. Wennberg, M. Buchwitz, R. de Beek, J. P. Burrows, D. Crisp, M. Christi, B. J. Connor, V. Natraj, and Y. L. Yung, "Space-based near-infrared CO_2 measurements: Testing the Orbiting Carbon Observatory retrieval algorithm and validation concept using SCIAMACHY observations over Park Falls, Wisconsin," J. Geophys. Res.: Atmos. **111**(D23), 1–17, doi:10.1029/2006JD007080 (2006).

[3] C. E. Miller, L. R. Brown, R. A. Toth, D. C. Benner, and V. M. Devi, "Spectroscopic challenges for high accuracy retrievals of atmospheric CO_2

and the Orbiting Carbon Observatory (OCO) experiment," C. R. Phys. **6**, 876–887 (2005).
[4]H. Boesch, D. Baker, B. Connor, D. Crisp, and C. Miller, "Global characterization of CO_2 column retrievals from shortwave-infrared satellite observations of the Orbiting Carbon Observatory-2 mission," Remote Sens. **3**, 270–304 (2011).
[5]L. Wang, V. Perevalov, S. Tashkun, Y. Ding, and S.-M. Hu, "Absolute line intensities of $^{13}C^{16}O_2$ in the 4200 ± 8500 cm^{-1} region," J. Mol. Spectrosc. **234**, 84–92 (2005).
[6]K. Song, S. Kassi, S. Tashkun, V. Perevalov, and A. Campargue, "High sensitivity *CW*-cavity ring down spectroscopy of $^{12}CO_2$ near 1.35 μm (II): New observations and line intensities modeling," J. Quant. Spectrosc. Radiat. Transfer **111**, 332–344 (2010).
[7]G. Casa, R. Wehr, A. Castrillo, E. Fasci, and L. Gianfrani, "The line shape problem in the near-infrared spectrum of self-colliding CO_2 molecules: Experimental investigation and test of semiclassical models," J. Chem. Phys. **130**, 184306 (2009).
[8]G. Casa, D. A. Parretta, A. Castrillo, R. Wehr, and L. Gianfrani, "Highly accurate determinations of CO_2 line strengths using intensity-stabilized diode laser absorption spectrometry," J. Chem. Phys. **127**, 084311 (2007).
[9]G. Wuebbeler, G. J. P. Viquez, K. Jousten, O. Werhahn, and C. Elster, "Comparison and assessment of procedures for calculating the R(12) line strength of the $\nu_1 + 2\nu_2 + \nu_3$ band of CO_2," J. Chem. Phys. **135**, 204304 (2011).
[10]O. L. Polyansky, K. Bielska, M. Ghysels, L. Lodi, N. F. Zobov, J. T. Hodges, and J. Tennyson, "High-accuracy CO_2 line intensities determined from theory and experiment," Phys. Rev. Lett. **114**, 243001 (2015).
[11]E. Zak, J. Tennyson, O. L. Polyansky, L. Lodi, N. F. Zobov, S. A. Tashkun, and V. I. Perevalov, "A room temperature CO_2 line list with *ab initio* computed intensities," in *XVIIIth Symposium on High Resolution Molecular Spectroscopy (HighRus-2015), Tomsk, Russia* [J. Quant. Spectrosc. Radiat. Transfer **177**, 31–42 (2016)].
[12]P. Amodio, L. Moretti, A. Castrillo, and L. Gianfrani, "Line-narrowing effects in the near-infrared spectrum of water and precision determination of spectroscopic parameters," J. Chem. Phys. **140**, 044310 (2014).
[13]J. Tennyson, P. F. Bernath, A. Campargue, A. G. Császár, L. Daumont, R. R. Gamache, J. T. Hodges, D. Lisak, O. V. Naumenko, L. S. Rothman, H. Tran, N. F. Zobov, J. Buldyreva, C. D. Boone, M. D. D. Vizia, L. Gianfrani, J.-M. Hartmann, R. McPheat, D. Weidmann, J. Murray, N. H. Ngo, and O. L. Polyansky, "Recommended isolated-line profile for representing high-resolution spectroscopic transitions (IUPAC technical report)," Pure Appl. Chem. **86**, 1931–1943 (2014).
[14]N. Ngo, D. Lisak, H. Tran, and J.-M. Hartmann, "An isolated line-shape model to go beyond the Voigt profile in spectroscopic databases and radiative transfer codes," J. Quant. Spectrosc. Radiat. Transfer **129**, 89–100 (2013).
[15]J. Morville, S. Kassi, M. Chenevier, and D. Romanini, "Fast, low-noise, mode-by-mode, cavity-enhanced absorption spectroscopy by diode-laser self-locking," Appl. Phys. B **80**, 1027–1038 (2005).
[16]R. Wehr, S. Kassi, D. Romanini, and L. Gianfrani, "Optical feedback cavity-enhanced absorption spectroscopy for *in situ* measurements of the ratio ^{13}C:^{12}C in CO_2," Appl. Phys. B **92**, 459 (2008).
[17]A. Castrillo, G. Gagliardi, G. Casa, and L. Gianfrani, "Combined interferometric and absorption-spectroscopic technique for determining molecular line strengths: Applications to CO_2," Phys. Rev. A **67**, 062503 (2003).
[18]F. Rohart, H. Mader, and H.-W. Nicolaisen, "Speed dependence of rotational relaxation induced by foreign gas collisions: Studies on CH_3F by millimeter wave coherent transients," J. Chem. Phys. **101**, 6475–6486 (1994).
[19]F. Rohart, A. Ellendt, F. Kaghat, and H. Mader, "Self and polar foreign gas line broadening and frequency shifting of CH_3F: Effect of the speed dependence observed by millimeter-wave coherent transients," J. Mol. Spectrosc. **185**, 222–233 (1997).
[20]L. Rothman, I. Gordon, Y. Babikov, A. Barbe, D. C. Benner, P. Bernath, M. Birk, L. Bizzocchi, V. Boudon, L. Brown, A. Campargue, K. Chance, E. Cohen, L. Coudert, V. Devi, B. Drouin, A. Fayt, J.-M. Flaud, R. Gamache, J. Harrison, J.-M. Hartmann, C. Hill, J. Hodges, D. Jacquemart, A. Jolly, J. Lamouroux, R. L. Roy, G. Li, D. Long, O. Lyulin, C. Mackie, S. Massie, S. Mikhailenko, H. Miller, O. Naumenko, A. Nikitin, J. Orphal, V. Perevalov, A. Perrin, E. Polovtseva, C. Richard, M. Smith, E. Starikova, K. Sung, S. Tashkun, J. Tennyson, G. Toon, V. Tyuterev, and G. Wagner, "The HITRAN2012 molecular spectroscopic database," J. Quant. Spectrosc. Radiat. Transfer **130**, 4–50 (2013).
[21]P. Amodio, M. D. De Vizia, L. Moretti, and L. Gianfrani, "Investigating the ultimate accuracy of Doppler-broadening thermometry by means of a global fitting procedure," Phys. Rev. A **92**, 032506 (2015).
[22]A. Malengo and F. Pennecchi, "A weighted total least-squares algorithm for any fitting model with correlated variables," Metrologia **50**, 654 (2013).
[23]N. Jacquinet-Husson, R. Armante, N. Scott, A. Chedin, L. Crepeau, C. Boutammine, A. Bouhdaoui, C. Crevoisier, V. Capelle, C. Boonne, N. Poulet-Crovisier, A. Barbe, D. C. Benner, V. Boudon, L. Brown, J. Buldyreva, A. Campargue, L. Coudert, V. Devi, M. Down, B. Drouin, A. Fayt, C. Fittschen, J.-M. Flaud, R. Gamache, J. Harrison, C. Hill, Ø. Hodnebrog, S.-M. Hu, D. Jacquemart, A. Jolly, E. Jimenez, N. Lavrentieva, A.-W. Liu, L. Lodi, O. Lyulin, S. Massie, S. Mikhailenko, H. Muller, O. Naumenko, A. Nikitin, C. Nielsen, J. Orphal, V. Perevalov, A. Perrin, E. Polovtseva, A. Predoi-Cross, M. Rotger, A. Ruth, S. Yu, K. Sung, S. Tashkun, J. Tennyson, V. Tyuterev, J. V. Auwera, B. Voronin, and A. Makie, "The 2015 edition of the GEISA spectroscopic database," J. Mol. Spectrosc. **327**, 31–72 (2016), New Visions of Spectroscopic Databases, Volume II.
[24]I. E. Gordon *et al.*, "The HITRAN2016 molecular spectroscopic database," J. Quant. Spectrosc. Radiat. Transfer (to be published).
[25]H. W. Yoon, J. J. Butler, T. C. Larason, and G. P. Eppeldauer, "Linearity of InGaAs photodiodes," Metrologia **40**, S154 (2003).
[26]M. D. De Vizia, A. Castrillo, E. Fasci, P. Amodio, L. Moretti, and L. Gianfrani, "Experimental test of the quadratic approximation in the partially correlated speed-dependent hard-collision profile," Phys. Rev. A **90**, 022503 (2014).
[27]G. Larcher, X. Landsheere, M. Schwell, and H. Tran, "Spectral shape parameters of pure CO_2 transitions near 1.6 μm by tunable diode laser spectroscopy," J. Quant. Spectrosc. Radiat. Transfer **164**, 82–88 (2015).